Polymer Journal (2011) 43, 41–50

www.nature.com/pj

ORIGINAL ARTICLE

Synthesis of thermoresponsive unimolecular polymeric micelles with a hydrophilic hyperbranched poly(glycidol) core

Shizhong Luo, Xianglong Hu, Yuanyuan Zhang, Congxiang Ling, Xi Liu and Shuaishuai Chen

This paper describes the reversible phase transition behavior of a thermoresponsive poly(*N*-isopropylacrylamide) (PNIPAM) shell at the surface of a hydrophilic core. Reversible addition-fragmentation transfer (RAFT) polymerization of *N*-isopropylacrylamide was conducted using a hydrophilic hyperbranched poly(glycidol) (HPG)-based macroRAFT agent. At lower temperatures ($<30\,^{\circ}C$), the resultant multiarm star block copolymer (HPG–PNIPAM) exists as unimolecular micelles, with hydrophilic HPG as the core and a densely grafted PNIPAM brush as the shell. In laser light scattering (LLS) studies, the concentration used for HPG–PNIPAM is $5\times10^{-6}\,g\,ml^{-1}$, to avoid any possible aggregation between dendritic unimolecular micelles above the lower critical solution temperature ($\sim32\,^{\circ}C$) of PNIPAM. What we observe for the phase transition of HPG–PNIPAM involves only unimolecular process. A combination of dynamic and static LLS studies of HPG–PNIPAM in aqueous solution reveals a reversible phase transition on heating and cooling.
Polymer Journal (2011) **43,** 41–50; doi:10.1038/pj.2010.93; published online 3 November 2010

Keywords: hyperbranched poly(glycidol); laser light scattering; unimolecular polymeric micelle

INTRODUCTION

It is well known that amphiphilic block copolymers can self-assemble into aggregates with various morphologies in water above the critical micelle concentration.[1–3] However, the microstructure of block copolymer micelles is not static because of the presence of dynamic exchange between assembled aggregates and individual unimers. The equilibrium between aggregates and unimers is governed by a delicate balance of weak intermolecular forces. The disruption of such a balance can be easily triggered by temperature, pH, dilution, salt concentration and so on.[4,5] The problem of insufficient stability of various aggregates can be addressed by structural fixation; for instance, chemical crosslinking of the micellar core or shell can lead to micelles with permanent stability.[6–11] On the other hand, to improve micelle stability, the synthesis of polymeric structures that mimic polymer micelles with regard to their morphological properties has been proposed recently.[12] Such polymers are referred to as unimolecular polymeric micelles and consist of covalently bound amphiphilic polymer chains. These colloids are also intrinsically stable on dilution, as their formation is independent of polymer concentration. Unimolecular polymeric micelles can be prepared from dendrimers, hyperbranched polymers, as well as from star polymers.[13–15] As we know, dendrimers are well-defined, highly branched macromolecules with hollow cores and dense shells.[16–25] Dendrimers show very interesting properties in the solid state and in solution because of their branching, globular shape, large modifiable surface functionality, as well as internal cavities. The special properties of dendritic boxes make them useful in many applications such as in drug release, molecular labels, probe moieties, chemical sensors, holographic data storage and molecular shuttles for transporting guest molecules between two different phases.[26–32] However, dendrimers are synthesized by complicated multistep reactions that limit their bulk applications. Hyperbranched polymers, which are the imperfect analogs of dendrimers, can be used as a potential alternative because they can be obtained conveniently in a single step and in high yield.[20,33–35] From a practical point of view, the amphiphilic hyperbranched macromolecules have potential practical applications.[36–38] Therefore, it is interesting to use hyperbranched polymers as the favorable starting materials for the synthesis of a globular amphiphile with unimolecular micellar properties.

Water-soluble polymers with thermosensitivity are of great scientific and technological importance and are extensively used as additives by pharmaceutical, cosmetic, food and paint industries.[39–41] Poly (*N*-isopropylacrylamide) (PNIPAM) is perhaps the most well-known member of the class of thermoresponsive polymers; it undergoes a phase transition at its lower critical solution temperature (LCST) of 32 °C and has been widely studied as a polymer that is potentially

Anhui Key Laboratory of Functional Molecular Solids and Anhui Key Laboratory of Molecule-based Materials, College of Chemistry and Materials Science, Anhui Normal University, Anhui, China
Correspondence: Dr S Luo, Anhui Key Laboratory of Functional Molecular Solids and Anhui Key Laboratory of Molecule-based Materials, College of Chemistry and Materials Science, Anhui Normal University, Wuhu, Anhui 241000, China.
E-mail: shzhluo@mail.ahnu.edu.cn
Received 30 March 2010; revised 1 September 2010; accepted 10 September 2010; published online 3 November 2010

useful for targeted drug delivery, solute separation, tissue culture substrate and controlling the adsorption of proteins.[42–46] You *et al.*[47] have achieved reversible switching between the dendritic hydrophobic core, a second-generation hyperbranched polyester Bolton H20, and the hydrophilic shell by grafting PNIPAM from the terminals of H20. Recently, we have synthesized unimolecular micelles with PNIPAM shell grafting from a hydrophobic fourth-generation hyperbranched polymester H40, and demonstrated their special phase transition behavior.[48]

Up to now, water-soluble hyperbranched poly(glycidol) (HPG) has been used widely to prepare amphiphilic molecular nanocapsules because it is highly biocompatible and without evident animal toxicity, which could encapsulate polar guests from water.[34,49–60] Peng *et al.*[50] have obtained star-hyperbranched block copolymers of HPG-*b*-polystyrene using atom transfer radical polymerization; these have good structural formation for ionic conductivity. Brooks *et al.*[60] have reported the use of amphiphilic HPG as nanoreators for unimolecular elimination reactions. Haag *et al.*[61] and Kono *et al.*[62] have functionalized HPG with pH responsiveness. Frey and co-workers[54,63] have already reported the synthesis and properties of an amphiphilic molecular nanocapsule consisting of an HPG core, whereas the same activity was not shown by linear polymers, suggesting that the encapsulation was related to the structure of the hyperbranched architecture. Recently, Satoh *et al.*[56] synthesized the HPG-bearing imidazolium tosylate units through the imidazolium salt modification of HPG. The modified HPG was found to possess novel LCST-type liquid–liquid and liquid–solid phase transition behaviors in a methanol/chloroform mixed solution.

To the best of our knowledge, it is rare to further study phase transition behavior of thermoresponsive chains tethered to a hydrophilic dendritic core, that is, HPG. Herein, we prepared unimolecular polymeric core-shell micelles with a hydrophilic HPG core and a temperature-responsive PNIPAM corona by means of the reversible addition-fragmentation transfer (RAFT) polymerization process. The themoresponsivity of PNIPAM corona is characterized in detail by dynamic and static laser light scattering (LLS). We demonstrate here that unimolecular polymeric micelles exhibit a reversible phase transition behavior on heating and cooling in dilute aqueous solutions.

EXPERIMENTAL PROCEDURE

Materials

Boron trifluoride diethyl etherate, glycerol and glycidol were obtained from Fluka (Shanghai, China) and were dried by refluxing over CaH_2 for 6 h under nitrogen, then distilled under vacuum. Bromobenzene, carbon disulfide and *N,N*-dimethyl formamide (DMF) were obtained from Aldrich (Shanghai, China) and were dried by refluxing over CaH_2 overnight, then distilled under reduced pressure and stored under nitrogen. *N*-isopropylacrylamide (NIPAM) was purified by recrystallization from benzene/*n*-hexane mixture. Tetrahydrofuran (THF) was distilled over sodium/ benzophenone before use. Other reagents were used as received.

Sample preparation

Scheme 1 shows general synthetic routes used for the synthesis of the core-shell structure (denoted as HPG–PNIPAM). The experimental details are described below.

Synthesis of HPG

HPG was synthesized by means of a one-pot process, according to the reported procedure.[49] For a typical procedure, glycerol (0.798 g, 8.6 mmol) and chloroform (80 ml) were mixed and stirred with a mechanical stirrer under nitrogen at −5 °C for 30 min. Subsequently, glycidol (28.6 g, 387 mmol) and boron trifluoride diethyl etherate (11.4 g, 80.3 mmol) were added dropwise for 1 h and were continuously reacted for 3 h. The mixture was neutralized, washed and purified. Most of the solvent and water were removed with a rotatory evaporator before precipitation into diethyl ether. HPG was further purified by precipitation into anhydrous diethyl ether from methanol three times. The product HPG was dried overnight under vacuum at 80 °C.

Synthesis of maleic anhydride (MAh) modified HPG

HPG (11.324 g, 3.3 mmol) was dissolved in dried DMF (90 ml), and then MAh (31 g, 316 mmol) was added. The mixture was stirred at 45 °C for 24 h. Most of the solvent was evaporated under reduced pressure before precipitation into dichloromethane. The crude product was further purified by precipitation into dichloromethane from DMF three times to remove any unreacted MAh. The resulting HPG–MAh was dried under vacuum at 40 °C overnight.

Synthesis of dithiobenzoic acid (DTBA)[64]

The Grignard reagent prepared from bromobenzene (31 g, 197 mmol) and magnesium (5.6 g, 230 mmol) in anhydrous THF (100 ml) was reacted with carbon disulfide (15 g, 197 mmol) in THF (50 ml) at 0 °C for 2 h, after which ice-cold dilute hydrochloric acid (0.01 M, 60 ml) was added dropwise. The organic layer was separated and extracted with 10% ice-cold sodium hydroxide solution (30 ml ×3). The alkaline solution was washed with diethyl ether, acidified with 10% hydrochloric acid solution and finally extracted with diethyl ether. The ether solution was washed with distilled water three times. After evaporation of the solvent, pure DTBA was obtained.

Synthesis of HPG macroRAFT agent

A solution of HPG–MAh (2.322 g, 0.29 mmol) and DTBA (3.860 g, 25 mmol) in anhydrous DMF was sealed in a Schlenk flask, and the reaction of DTBA with HPG–MAh was carried out at 60 °C for 24 h; HPG capped with dithiobenzoate groups was obtained by precipitation into diethyl ester from DMF three times. The resulting macroRAFT agent was dried in a vacuum oven at 60 °C overnight.

Synthesis of HPG–PNIPAM

The general procedure for synthesizing HPG–PNIPAM was as follows: a Schlenk flask was charged with an HPG-based macroRAFT agent (0.1 g, 6.44×10^{-3} mmol), azobisisobutyronitrile (AIBN) (0.013 g, 0.08 mmol) and NIPAM (8.736 g, 77.3 mmol) in anhydrous DMF, then degassed by three freeze–thaw cycles and sealed under vacuum. Polymerization was carried out at 80 °C for 24 h. The mixture was precipitated into anhydrous diethyl ester from DMF three times. The product was collected by filtration and then dried in a vacuum oven at 60 °C overnight.

Cleavage of grafted PNIPAM chains[48]

A volume of 0.302 g (3.96×10^{-4} mmol) of HPG–PNIPAM was dissolved in 50 ml of anhydrous THF, and excess lithium chloride (0.008 g, 0.19 mmol) and potassium borohydride (0.010 g, 0.19 mmol) were slowly added to the solution. The reaction was refluxed with vigorous stirring under nitrogen until the evolution of gas ceased. The salts contained in the resulting solution were removed by filtering in an aluminum oxide column. After concentrating the solution, it was precipitated in hot water (40 °C) three times. The cleaved thiol end PNIPAM was dried in a vacuum oven at room temperature overnight. The above reduction procedure degraded the ester bonds and recovered the grafted PNIPAM for further size exclusion chromatography (SEC) measurement.

Measurements

Nuclear magnetic resonance (NMR) spectroscopy. ^{1}H NMR and ^{13}C NMR spectra were recorded using a Bruker 300 MHz spectrometer (Bruker BioSpin, Rheinstetten, Germany). HPG and HPG–PNIPAM were analyzed in D_2O, and HPG–MAh, DTBA and macroRAFT agent were analyzed in CD_3OD, $CDCl_3$ and dimethyl sulfoxide (DMSO)-d_6, respectively.

Fourier transform infrared measurements. Fourier transform infrared spectra were collected at 64 scans with a spectral resolution of 4 cm^{-1} on a Shimadzu IR Prestige-21 spectrometer (Shimadzu Corporation, Tokyo, Japan) with KBr.

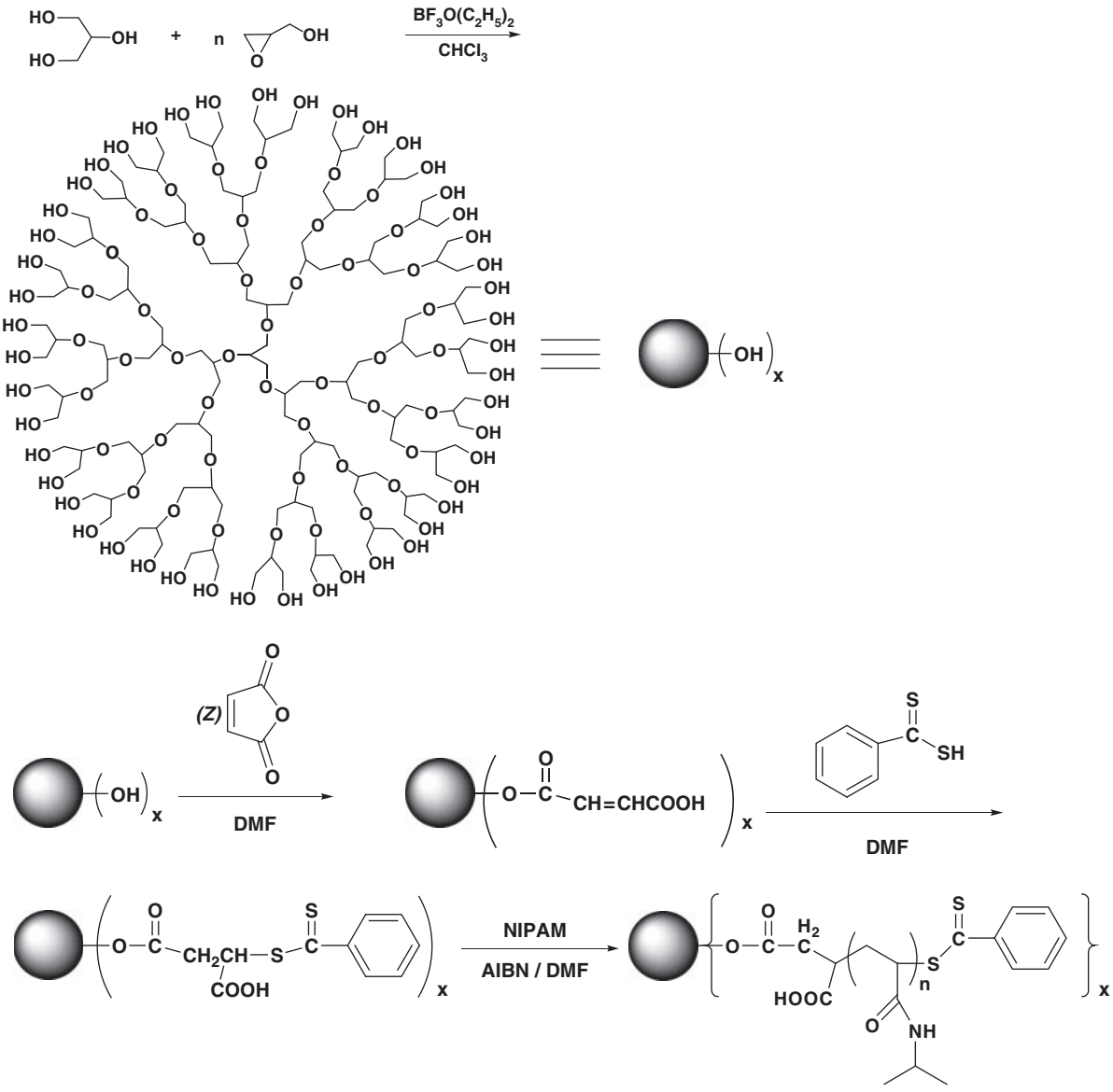

Scheme 1 Schematic illustration for the preparation of hyperbranched poly(glycidol)–poly(*N*-isopropylacrylamide). DMF, dimethyl formamide; NIPAM, *N*-isopropylacrylamide.

Elemental analysis. Elemental analyses for HPG, HPG–MAh and HPG macroRAFT agent were performed with a Vario EL III CHNS/O analyzer (Elementar Corporation, Hanau, Germany).

Thermogravimetric analysis. Thermogravimetric analysis was performed in argon at a heating rate of 10 °C min^{-1} from room temperature to 600 °C using a Shimadzu DTG-60.

Size exclusion chromatography. Molecular weights and molecular weight distributions were determined by SEC on an instrument equipped with a Waters 1515 pump and a Waters 2414 differential refractive index detector (set at 35 °C). Three Styragel columns connected in series, HR2, HR3 and HR6, were used at an oven temperature of 35 °C. The eluent was THF at a flow rate of 1.0 ml min^{-1}. A series of low-polydispersity polystyrene standards were used for the calibration.

Temperature-dependent turbidimetry. The optical transmittance of the aqueous solution was acquired on a Unico UV/vis 2802PCS spectrophotometer (Unico Instrument Co., Ltd., Shanghai, China) and measured at a wavelength of 600 nm using a thermostatically controlled cuvette.

Scanning electron microscopy (SEM). SEM observations were conducted on a Hitachi S-4800 Field Emission Scanning Electron Microscope at room temperature. The sample for SEM images was prepared by vacuum evaporation of unimolecular micelles aqueous solution at 40 °C overnight, then coated with platinum.

Laser light scattering. A commercial spectrometer (ALV/DLS/SLS-5022F, ALV GmbH, Langen, Germany) equipped with a multitau digital time correlation (ALV5000) and a cylindrical 22 mW UNIPHASE He-Ne laser (λ_0=632 nm) as the light source was used. In static LLS, we can obtain the weight-average molar mass (M_w) and the *z*-average root-mean square radius of gyration ($\langle R_g^2 \rangle^{1/2}$ or written as $\langle R_g \rangle$) of polymer chains in a dilute solution from the angular dependence of the excess absolute scattering intensity, known as Rayleigh ratio $R_{vv}(q)$, as

$$\frac{KC}{R_{vv}(q)} \approx \frac{1}{M_w}\left(1+\frac{1}{3}<R_g^2>q^2\right)+2A_2C \qquad (1)$$

where $K=4\pi^2n^2(dn/dC)^2/(N_A\lambda_0^4)$ and $q=(4\pi n/\lambda_0)\sin(\theta/2)$ with N_A, dn/dC, n and λ_0 being the Avogadro number, the specific refractive index increment,

the solvent refractive index and the wavelength of the laser light in a vacuum, respectively, and A_2 is the second virial coefficient. The specific refractive index increment (d*n*/d*C*) was determined by a precise differential refractometer at 632 nm. Sodium chloride (NaCl) aqueous solution was used for calibrating the refractometer. The experimental setup and basic theory have been detailed previously.[65] The obtained d*n*/d*C* of HPG and HPG–PNIPAM in water at 25 °C were 0.131 and 0.164 ml g^{-1}, respectively. Strictly speaking, here, $R_{vv}(q)$ should be $R_{vu}(q)$ because there is no analyzer before the detector. However, the depolarized scattering of the solution studied is insignificant so that $R_{vu}(q) \sim R_{vv}(q)$. It is to be noted further that, in this study, the sample solution was so dilute (5×10^{-6} g ml^{-1}) that the extrapolation of $C\rightarrow0$ was not necessary, and the term $2A_2C$ in Equation 1 can be neglected.

In dynamic LLS, the Laplace inversion of each measured intensity–intensity–time correlation function $G^{(2)}(q,t)$ in the self-beating mode can lead to a linewidth distribution $G(\Gamma)$. For a pure diffusive relaxation, Γ is related to the translational diffusion coefficient D by $(\Gamma/q^2)_{C\rightarrow0,q\rightarrow0}\rightarrow D$, or further to the hydrodynamic radius $\langle R_h \rangle$ by the Stokes–Einstein equation, $\langle R_h \rangle = (k_BT/6\pi\eta_0)/D$, where k_B, T and η_0 are the Boltzmann constant, the absolute temperature and the solvent viscosity, respectively.

RESULTS AND DISCUSSION

Synthesis of HPG–PNIPAM

The procedure to prepare HPG–PNIPAM is shown in Scheme 1. It is worth noting that the chemical structure of HPG described in Scheme 1 is an ideal dendrimer containing 48 primary hydroxyl groups and a molar mass of 3423 g mol^{-1}, according to the theoretical model from its preparation reaction.[49,54,62] Results of elemental analysis were as follows: calculated for HPG: C, 48.38; H, 8.18. Found: C, 46.06; H, 8.33. ^{13}C NMR (D_2O) of HPG: δ=62.56 (secondary carbon with terminated hydroxyl, –CH_2–OH), 71.74 (secondary carbon, –CH_2–O–), 82.43 (tertiary carbon, –O–CH $(CH_2OH)_2$), 80.60 p.p.m. (tertiary carbon, –O–CH $(CH_2)_2$–). Generally, ^{13}C NMR is used to characterize the hyperbranched polymer. According to Žagar *et al.*,[66] the degree of branching of HPG was 0.57 and the average number of monomeric units (the degree of polymerization) was ∼45.

The HPG macroRAFT agent was prepared by a two-step approach.[64] First, hydroxyl-terminated HPG was reacted with MAh in DMF to form MAh-terminated HPG. Second, DTBA was added onto the double bond of the HPG–MAh to produce dithiobenzoate-terminated HPG, namely, HPG macroRAFT agent. ^{1}H NMR spectra (*a*), (*b*) and (*c*) in Figure 1 show the HPG, HPG–MAh and HPG macroRAFT agent, respectively. For the spectrum of HPG–MAh in CD_3OD, the signals at δ=∼4.2 and 6.2–6.4 p.p.m. correspond to all the ester methylene protons and protons of double bonds from the maleic acid monoester groups, respectively. According to the integral area ratio of these two peaks, the number of maleic acid monoester groups per HPG–MAh is calculated to be ∼45, which is consistent with the average number of monomeric units (the degree of polymerization) of HPG. Because of the strong acidity of DTBA compared with maleic acid monoester, it can easily react with the double bond to prepare the corresponding HPG macroRAFT agent. From spectrum

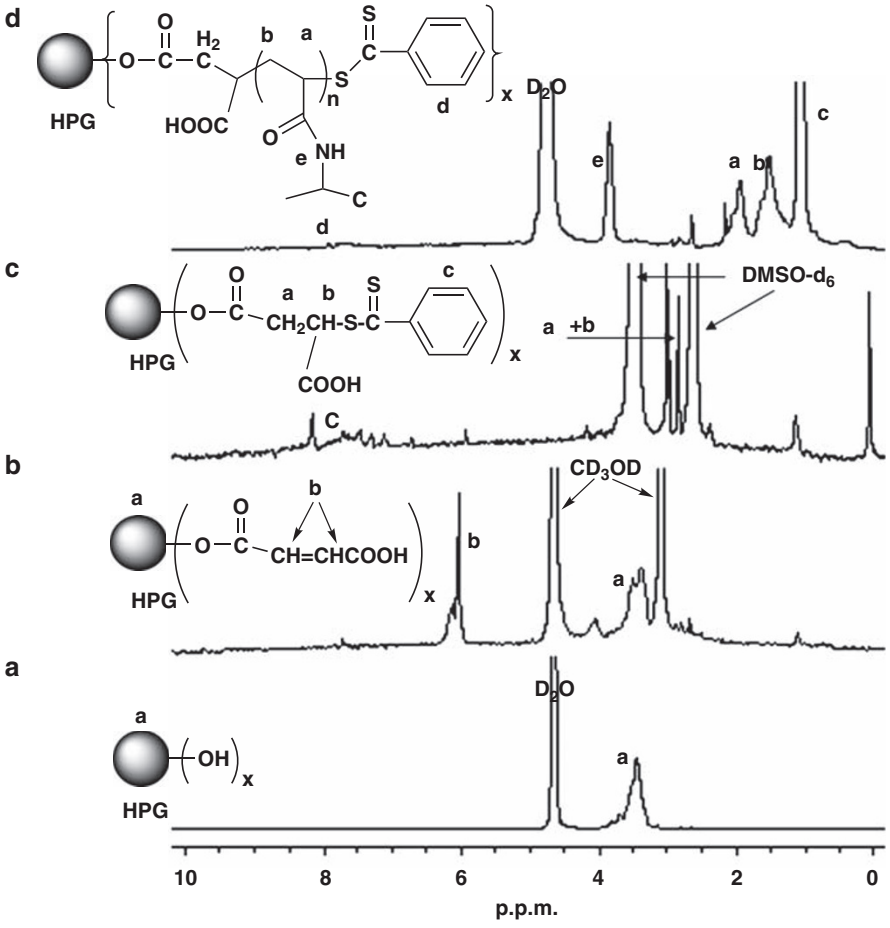

Figure 1 ^{1}H nuclear magnetic resonance spectra of (**a**) HPG in D_2O, (**b**) HPG–maleic anhydride in CD_3OD, (**c**) HPG macro-reversible addition-fragmentation transfer agent in DMSO-d_6 and (**d**) HPG–poly(*N*-isopropylacrylamide) in D_2O. HPG, hyperbranched poly(glycidol); DMSO, dimethyl sulfoxide.

(*c*) in Figure 1, the disappearance of signals at δ=6.2–6.4 p.p.m. and the appearance of new signals at δ=7.3, 7.6 and 7.9 p.p.m., ascribed to the *meta*-, *para*- and *ortho*-position protons of the dithilbenzoyl group, respectively, confirm the successful preparation of the HPG macroRAFT agent. Elemental analyses and ^{13}C NMR spectra further confirmed their chemical structures. Results of elemental analysis were as follows: calculated for HPG–MAh: C, 48.73; H, 4.60. Found: C, 47.77; H, 4.76. Calculated for HPG macroRAFT agent: C, 51.50; H, 4.26; S, 19.80. Found: C, 50.30; H, 4.99, S, 19.27. In the ^{13}C NMR (CD_3OD) of HPG–MAh, new signals of δ=133.08 (allyl, –*CH*=), 132.76 (allyl, =*CH*–COOH), 169.57 (carboxyl, –*COOH*) and 165.33 p.p.m. (carbonyl, –O–*CO*–CH=) indicate the formation of HPG–MAh. In the ^{13}C NMR (DMSO-d_6) of HPG macroRAFT agent, the disappearance of signals of δ=133.08 (allyl, –*CH*=) and 132.76 p.p.m. (allyl, =*CH*–COOH) and the new signals of δ=32.57 (methylene, –OCO–CH_2–) and 41.86 p.p.m. (methylidyne, –*CH*(COOH)–) approve the resulting HPG macroRAFT agent.

RAFT polymerization of NIPAM was performed in a sealed Schlenk flask under vacuum using HPG macroRAFT agent to prepare a dendritic core-shell nanostructure with HPG as the dendritic hydrophilic core and PNIPAM as the shell. You *et al.*[47] and Liu *et al.*[64] have investigated the RAFT polymerization of NIPAM from a dendrimer and found that RAFT polymerization of NIPAM can be carried out in a controlled manner. Therefore, we did not study in detail the kinetics of RAFT polymerization of NIPAM using HPG macroRAFT agent. ^1H NMR spectrum (*d*) of HPG–PNIPAM in D_2O in Figure 1 reveals the presence of PNIPAM characteristic signals at δ= ~1.2 and 4.0 p.p.m.

To further confirm the successful RAFT polymerization of NIPAM, we recorded the Fourier transform infrared spectroscopy of HPG macroRAFT agent and HPG–PNIPAM in Figure 2. On the basis of spectrum (*a*) in Figure 2, the characteristic absorption peaks of phenyl and carbonyl located at 1400–1600 cm^{-1} and 1730 cm^{-1}, respectively, once again support the prepared HPG macroRAFT agent. Contradistinctively, the representative peaks of isopropyl groups at 2962 cm^{-1} and 2872 cm^{-1}, as well as the *N–H* bond stretching at 3300 cm^{-1}, clearly indicate the synthesized HPG–PNIPAM from the spectrum (*b*) in Figure 2.

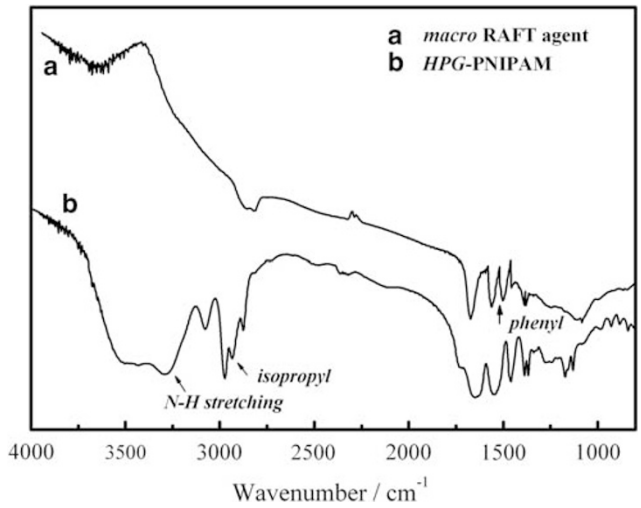

Figure 2 Fourier transform infrared spectra recorded for (**a**) HPG-based macroRAFT agent and (**b**) HPG–PNIPAM. HPG, hyperbranched poly(glycidol); PNIPAM, poly(*N*-isopropylacrylamide); RAFT, reversible addition-fragmentation transfer.

Figure 3 shows SEC traces recorded for HPG and HPG–PNIPAM. HPG–PNIPAM gives a symmetric elution peak with a number-average molecular weight (M_n) of 7.63×10^5 g mol^{-1} and a polydispersity of 1.23. The relatively narrow polydispersity of HPG–PNIPAM reveals the characteristic of controlled RAFT polymerization of NIPAM. Because of the fact that SEC analysis uses linear polystyrene as standards and HPG–PNIPAM takes a dendritic conformation, SEC tends to underestimate the molecular weight.[47] Therefore, the static LLS was used to measure the absolute molecular weight of HPG and HPG–PNIPAM.

In the LLS experiment, the angular dependence of the excess absolute time-averaged scattered light intensity, known as the excess Rayleigh ratio $R_{vv}(q)$, of dilute polymer solutions led to the weight-average molar mass M_w and $\langle R_g \rangle$ using a Zimm plot. In this study, the extrapolated value of $[R(q)/KC]_{q\to0}$ leads to an apparent $M_{w,app}$, which, because of the very low concentration used (5×10^{-6} g ml^{-1}), is likely to be close to the absolute M_w of the polymer. It is reasonable that the extrapolation to zero concentration was not carried out because of the small concentration effect in the very dilute regime. Figure 4 shows scattering vector (q) dependence of Rayleigh ratio $R_{vv}(q)$ of HPG and HPG–PNIPAM in aqueous solution at 20 °C. On the basis of Equation (1) and Figure 4, the $M_{w,app}$ values of HPG and HPG–PNIPAM determined in water are 4.8×10^3 and 1.3×10^6 g mol^{-1}, respectively. The $\langle R_g \rangle$ values of HPG and HPG–PNIPAM are 6.84 and 101.6 nm, respectively. In dilute solution, the second virial coefficient A_2 indicates the interaction between

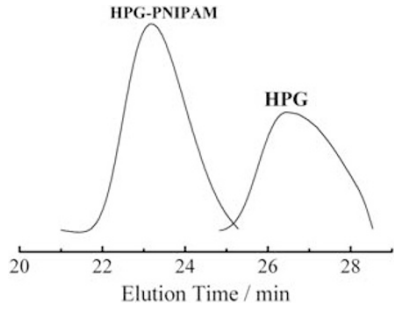

Figure 3 Gel permeation chromatography (GPC) traces recorded for hyperbranched poly(glycidol) (HPG) and HPG–PNIPAM (poly(*N*-isopropylacrylamide)).

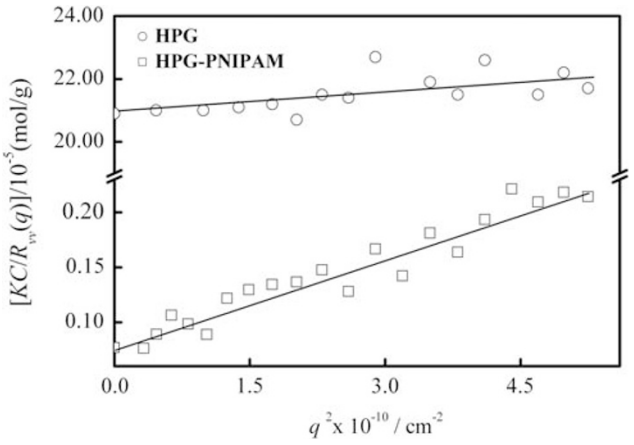

Figure 4 Scattering vector (q) dependence of the Rayleigh ratio $R_{vv}(q)$ of HPG (hyperbranched poly(glycidol)) and HPG-PNIPAM (poly(*N*-isopropylacrylamide)) in aqueous solution at 20 °C, wherein each concentration is 5×10^{-6} g ml^{-1}.

the solvent and the polymer. Here, the values of A_2 for HPG and HPG–PNIPAM are 2.5×10^{-4} and 1.08×10^{-2}, respectively. They are all above zero, approving intermolecular forces between the water and polymer over intramolecular interactions in this scenario. The A_2 of HPG–PNIPAM is greater than that of HPG; this indicates that HPG–PNIPAM appears more swollen and occupies a larger volume after being grafted with PNIPAM in water.

To determine the actual molecular weight of PNIPAM chains and the number of grafting arms, PNIPAM was cleaved from HPG–PNIPAM through reduction and purification, and SEC analysis of the recovered PNIPAM revealed an M_n of $2.56\times10^4\,g\,mol^{-1}$ and a polydispersity of 1.18. The degree of polymerization of PNIPAM was then calculated to be ~227. Considering that the $M_{w,app}$ of HPG–PNIPAM is $1.3\times10^6\,g\,mol^{-1}$ and the weight-average molar mass M_w of grafted PNIPAM chain is $3.02\times10^4\,g\,mol^{-1}$, the number of PNIPAM arms grafted per HPG core is calculated to be ~42. There are about 45 hydroxyl groups on the surface of HPG; therefore, ~93% of terminal-functionalized RAFT groups participated in the polymerization, assuming 100% functionalization of HPG during preparation of the macroRAFT agent. The molecular parameters of HPG and HPG–PNIPAM are summarized in Table 1.

It is worthy of note, as shown in Figure 5, that the decomposition temperature increases from 310 to 335 °C after being grafted with PNIPAM, suggesting the improved thermal stability of HPG. Wei *et al.*[52] also reported that the crosslinked HPG by terminal modification had a more thermal stability. Hopefully, HPG–PNIPAM can be used in a broad range of applications as a functionalized polymer.

Thermoresponsivity of unimolecular polymeric micelles

It is well known that the PNIPAM homopolymer undergoes a coil-to-globule phase transition in dilute aqueous solution at its LCST of ~32 °C.[46,67] At a temperature below LCST, PNIPAM chains take a random coil conformation because of the predominantly intermolecular hydrogen bonding between PNIPAM chains and water molecules. At a temperature above LCST, intramolecular hydrogen-bonding interactions between C=O and N–H groups render the chains to become compact and collapse, reducing their water solubility.

Figure 6 shows the temperature dependences of the transmittances of HPG–PNIPAM at different concentrations. For the concentration of $1\times10^{-3}\,g\,ml^{-1}$, it can be clearly seen that HPG–PNIPAM exhibits thermoresponsive aggregation at a temperature above LSCT of PNIPAM and the solution increases opaque. Above 34 °C, the transmittance stabilizes out, suggesting complete thermoinduced aggregation. Figure 6 also reveals that, for the concentration of $5\times10^{-6}\,g\,ml^{-1}$, transmittance remains constant at about 100% in the whole temperature range of 20–40 °C. It indicates that there is no aggregation during the collapse of PNIPAM shell at this concentration. Therefore, this concentration was selected to be used for taking LLS measurements in order to observe unimolecular phase transition of HPG–PNIPAM.

LLS was used to characterize the chain conformational changes of HPG–PNIPAM unimolecular micelles in aqueous solution on heating and cooling. The sample solution was clarified with 0.45 μm Millipore PTFE filter (Millipore Corporation, Bedford, MA, USA) to remove dust. Each data point was obtained after the measured values were stable, and it generally took 30 min for each temperature equilibration. Figure 7 shows temperature dependence of $\langle R_h \rangle$ and $M_{w,app}$ for HPG–PNIPAM, in which the concentration is $5\times10^{-6}\,g\,ml^{-1}$. The values of $M_{w,app}$ for HPG–PNIPAM remain nearly constant on heating

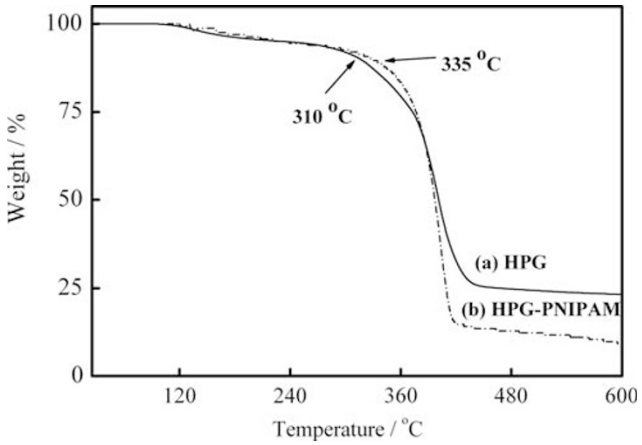

Figure 5 Thermogravimetric analysis curves of (**a**) HPG (hyperbranched poly(glycidol)) and (**b**) HPG–PNIPAM (poly(*N*-isopropylacrylamide)).

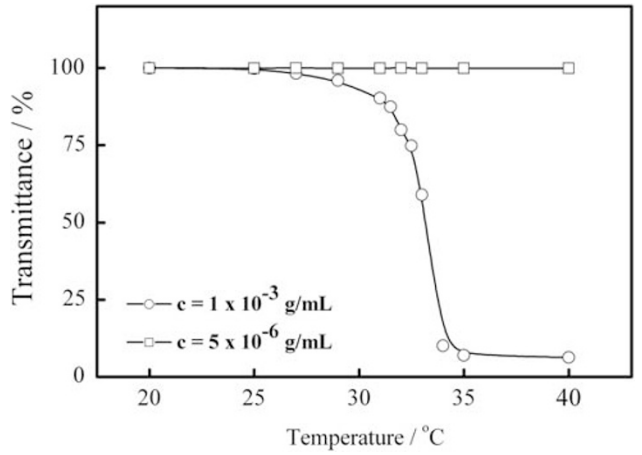

Figure 6 Temperature dependence of optical transmittance at 600 nm obtained for the different concentrations of hyperbranched poly(glycidol)–poly(*N*-isopropylacrylamide) aqueous solution.

Table 1 Molecular parameters of HPG and HPG–PNIPAM

Samples	M_n *g mol*$^{-1}$[a]	M_w/M_n[a]	$M_{w,app}$ *g mol*$^{-1}$[b]	$M_{n,\ PNIPAM}$ *g mol*$^{-1}$[c]	M_w/M_n[c]	*DP of PNIPAM*	*Number of arms*[d]
HPG	3.20×10^3	1.41	4.8×10^3	—	—	—	—
HPG–PNIPAM	7.63×10^5	1.23	1.3×10^6	2.56×10^4	1.18	227	42

Abbreviations: DP, degree of polymerization; HPG, hyperbranched poly(glycidol); PNIPAM, poly(*N*-isopropylacrylamide).
[a]Determined by size exclusion chromatography (SEC).
[b]Determined in water by static laser light scattering (LLS).
[c]Determined by SEC after cleavage via reduction with LiBH4.
[d]Calculated from $M_{w,app}$ determined by LLS and molecular weight of cleaved PNIPAM arms determined by SEC.

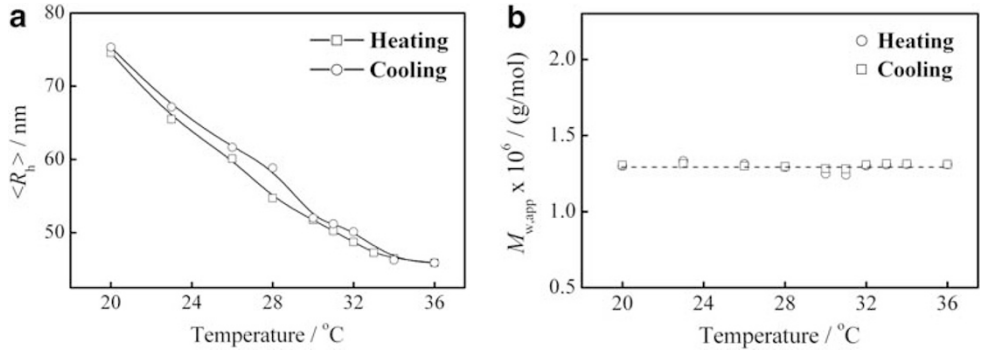

Figure 7 Temperature dependence of $\langle R_h \rangle$ of hyperbranched poly(glycidol)–poly(*N*-isopropylacrylamide) (**a**) and its $M_{w,app}$ (**b**), wherein the concentration is 5×10^{-6} g ml^{-1}.

and cooling in Figure 7b, indicating that there is no aggregation between dendritic unimolecular micelles at the concentration of 5×10^{-6} g ml^{-1}. Therefore, for the LLS measurements, what we observe for the phase transition of HPG–PNIPAM involves only unimolecular process.

For HPG–PNIPAM in Figure 7a, $\langle R_h \rangle$ decreases gradually from 75 to 46 nm in the broad temperature range of 20–34 °C and remains constant at 34–36 °C on heating because of the grafted PNIPAM chain shrinking, although it is well known that, for PNIPAM, homopolymer chain $\langle R_h \rangle$ drops sharply in the narrow temperature range of 31–33 °C.[46] Theoretical prediction suggests that strong interchain interactions are present in the brush and cause a broadening of the transition of polymer chains. Our previous works[48,64] and several experimental results[68–75] have already confirmed this prediction. As we know, when PNIPAM chains are attached by one end to a flat substrate or curved interface with sufficient density, referred to as a polymer brush, they are crowned and forced to stretch away from the surface to avoid overlapping. In our case, the molecular size of HPG is estimated to be ~3 nm;[35,66,76] the grafting of 42 PNIPAM chains from the HPG core results in a densely packed PNIPAM brush surrounding the hydrophilic core and the grafting density can be calculated as ~0.67 nm^2 per chain. Therefore, for HPG–PNIPAM, because of the grafted chain crowding and steric repulsion of neighboring chains in the brush, the results of dynamic LLS show a broad phase transition range from 20 to 34 °C. This is also in agreement with the theoretical prediction.[77] At 36 °C, the values of A_2 for HPG and HPG–PNIPAM are 2.47×10^{-4} and 3.33×10^{-3}, respectively. The A_2 of HPG–PNIPAM decreases as the solution temperature increases, a characteristic of aqueous polymer solution because of the negative entropy change; namely, A_2 of HPG–PNIPAM becomes lower as temperature increases because of the change in solvation; this indicates that HPG–PNIPAM appears to shrink more and occupies a smaller volume during temperature increase in water.

Conversely, because of the shell expanding, $\langle R_h \rangle$ increases from 46 to 75 nm as the temperature decreases from 36 to 20 °C in Figure 7a. This reveals that the phase transition behavior of the unimolecular polymeric micelles is completely reversible in the heating and cooling cycle. This kind of unimolecular polymeric micelles, in principle, has a number of nanomaterials applications, including drug release, diagnostics, catalysis and separation.

Figure 8 shows scattering vector (q) dependence of the average characteristic linewidth (Γ) of HPG–PNIPAM in aqueous solution at 20 and 36 °C, when the concentration is 5×10^{-6} g ml^{-1}. It reveals that the Γ is a linear function of q^2 and the extrapolation of Γ to $q\rightarrow0$ passes the origin, confirming that the apparent diffusion coefficient

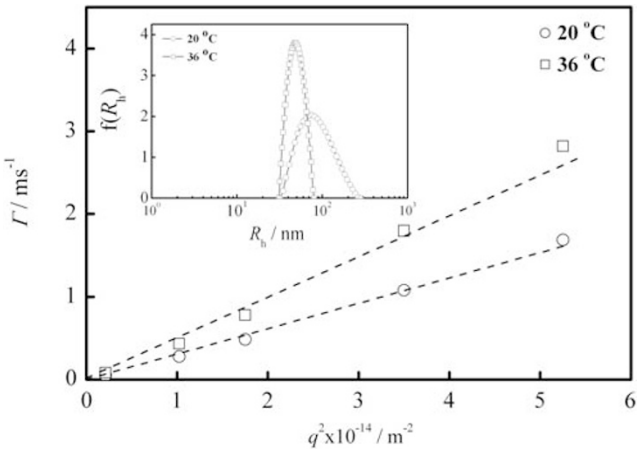

Figure 8 Scattering vector (q) dependence of the average characteristic linewidth (Γ) of hyperbranched poly(glycidol)–poly(*N*-isopropylacrylamide) (HPG–PNIPAM) in aqueous solution at 20 and 36 °C, wherein the concentration is 5×10^{-6} g ml^{-1}. The inset shows the corresponding hydrodynamic radius distributions f(R_h) of HPG–PNIPAM.

depends only on the translational motion during the heating process. The inset in Figure 8 shows typical hydrodynamic radius distributions f(R_h) of HPG–PNIPAM aqueous solution at 20 and 36 °C. It can be clearly seen that the distribution curve shifts to the left with increasing temperature. The average hydrodynamic radii $\langle R_h \rangle$ of HPG–PNIPAM at 20 and 36 °C are 75 and 46 nm, respectively. This should be ascribed to the collapsing of the PNIPAM brush. The monomodal distribution curves indicate that the unimolecular polymerice micelles are relatively monodisperse at different temperatures. The polydispersity indexes of the size distributions (μ_2/Γ^2) at 20 and 36 °C are 0.12 and 0.08, respectively.

The morphology of unimolecular polymeric micelles is shown in Figure 9. Approximately spherical nanoparticles with a mean diameter of 80 nm are observed. A closer examination of the SEM image reveals that some unimolecular micelles seem to be in contact with each other, possible because of the concentration and drying effects during sample preparation for SEM. The size is in reasonable agreement with the dynamic LLS results of HPG–PNIPAM if polydispersity and solvation effects are taken into account.

It is well known that the ratio of $\langle R_g \rangle/\langle R_h \rangle$ reflects the conformation of a polymer chain or the density distribution of chain segments in core-shell nanoparticles. A smaller value of

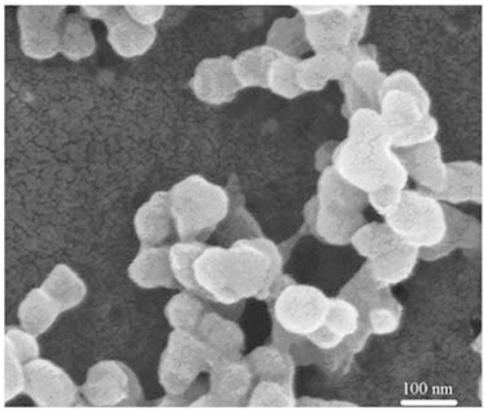

Figure 9 Typical scanning electron microscopy image of hyperbranched poly(glycidol)–poly(*N*-isopropylacrylamide) unimolecular micelles.

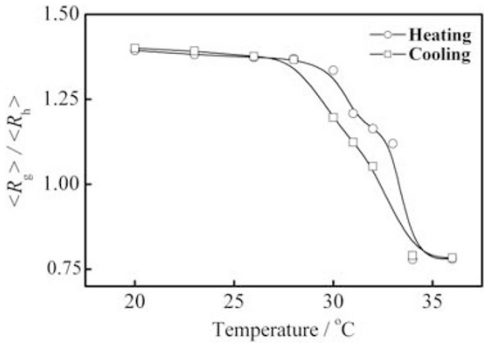

Figure 10 Temperature dependence of $\langle R_g \rangle / \langle R_h \rangle$ for aqueous solution of hyperbranched poly(glycidol)–poly(*N*-isopropylacrylamide) during the heating and cooling process, wherein the concentration is 5×10^{-6} g ml^{-1}.

$\langle R_g \rangle / \langle R_h \rangle$ typically hints at a higher chain segment density. For example, for linear and flexible polymer chains, $\langle R_g \rangle / \langle R_h \rangle$ is around 1.5, but for a uniform nondraining sphere, $\langle R_g \rangle / \langle R_h \rangle$ drops to 0.774. A ratio of 0.8–1.5 is found for hyperbranched or dendritic macromolecules.[78] Figure 10 shows the typical temperature dependences of $\langle R_g \rangle / \langle R_h \rangle$ for aqueous solution of HPG–PNIPAM during the heating and cooling process. The change of $\langle R_g \rangle / \langle R_h \rangle$ between $\sim$1.4 at 20 and $\sim$0.8 at 36 °C clearly indicates the grafted PNIPAM chains shrinking from an extended coil conformation to a collapsing state. This reversible phase transition behavior is illustrated in Scheme 2. The difference between the $\langle R_h \rangle$ dependence on temperature for HPG–PNIPAM in Figure 7 and the $\langle R_g \rangle / \langle R_h \rangle$ dependence on temperature in Figure 10 is understandable because they are defined in quite different ways. $\langle R_h \rangle$ is only the radius of an equivalent hard sphere that has an identical diffusion coefficient D as the polymer micelles in the solution, whereas $\langle R_g \rangle / \langle R_h \rangle$ depends only on the chain conformation. Figure 10 shows that when temperature is below 28 °C, $\langle R_g \rangle / \langle R_h \rangle$ is a constant ($\sim$1.4), even though $\langle R_h \rangle$ decreases with increasing temperature as shown in Figure 7a. This reveals that when the temperature is below the LCST of PNIPAM, the grafting PNIPAM chains in water behave in the manner of a random coil and the conformation is independent of temperature. Figure 10 shows also that, when the temperature is close to LCST of PNIPAM, $\langle R_g \rangle / \langle R_h \rangle$ decreases dramatically with increasing temperature because of the chain collapsing of PNIPAM. In our previous work,[48] PNIPAM brush, densely grafted at the surface of the hydrophobic hyperbranched H40 core, exhibits double thermal phase transition behavior. The collapsing of the PNIPAM brush occurs at lower temperatures (below 30 °C) and is ascribed to the fact that it is attached to a hydrophobic core. As we all know, when NIPAM monomer are block or randomly copolymerized with a hydrophilic or hydrophobic monomer, its LCST will increase or decrease to some extent.[42] Therefore, in this study, it is reasonable

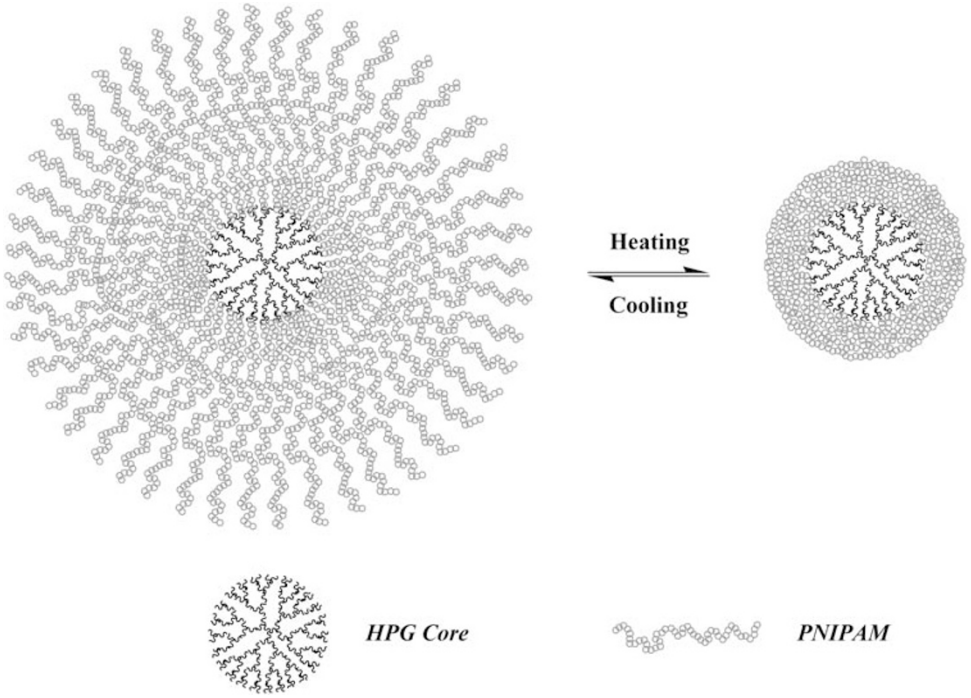

Scheme 2 Schematic illustration for the collapse and swelling of HPG–PNIPAM unimolecular micelles in water. HPG, hyperbranched poly(glycidol); PNIPAM, poly(*N*-isopropylacrylamide).

that the more noticeable phase transition occurs at temperatures above 30 °C (Figure 10), because of the hydrophilicity of the HPG core.

CONCLUSION

The hydrophilic hyperbranched polyglycidol (HPG) was synthesized by ring-opening polymerization in a one-pot process. RAFT polymerization of *N*-isopropylacrylamide (NIPAM) was conducted using an HPG-based macroRAFT agent. In aqueous solution, dendritic HPG–PNIPAM exists as unimolecular micelles, with hydrophilic HPG as the core and grafted PNIPAM chains as the shell. The prepared unimolecular polymeric micelles exhibit a reversible phase transition behavior during a heating and cooling cycle; this was confirmed by dynamic and static LLS measurements. Because of HPG combining several remarkable features, including a highly flexible aliphatic polyether backbone, hydrophilic groups and excellent biocompatibility, the HPG–PNIPAM unimolecular polymeric micelles are promising nanostructures for a variety of applications ranging from catalysts to drug delivery and controlled release.

ACKNOWLEDGEMENTS

The financial support of the National Natural Scientific Foundation of China (20704001), the Anhui Provincial Natural Science Foundation (070414191) and the Project of Scientific Research for Young University Teachers of Anhui Province (2007jq1059) is gratefully acknowledged.

1 Zhang, L. F. & Eisenberg, A. Multiple morphologies of crew-cut aggregates of polystyrene-*b*-poly(acrylic acid) block-copolymers. *Science* **268,** 1728–1731 (1995).
2 Du, J. Z., Tang, Y. P., Lewis, A. L. & Armes, S. P. pH-sensitive vesicles based on a biocompatible zwitterionic diblock copolymer. *J. Am. Chem. Soc.* **127,** 17982–17983 (2005).
3 Liu, S. Y., Billingham, N. C. & Armes, S. P. A schizophrenic water-soluble diblock copolymer. *Angew. Chem., Int. Ed.* **40,** 2328–2331 (2001).
4 Liu, S. Y., Ma, Y. H. & Armes, S. P. Direct verification of the core-shell structure of shell cross-linked micelles in the solid state using X-ray photoelectron spectroscopy. *Langmuir* **18,** 7780–7784 (2002).
5 Lee, A. S., Butun, V., Vamvakaki, M., Armes, S. P., Pople, J. A. & Gast, A. P. Structure of pH-dependent block copolymer micelles: charge and ionic strength dependence. *Macromolecules* **35,** 8540–8551 (2002).
6 Zheng, G., Zheng, Q. & Pan, C. One-pot synthesis of micelles with a cross-linked poly(acrylic acid) core. *Macromol. Chem. Phys.* **207,** 216–223 (2006).
7 Jiang, X. Z., Luo, S. Z., Armes, S. P., Shi, W. F. & Liu, S. Y. UV irradiation-induced shell cross-linked micelles with pH-responsive cores using ABC triblock copolymers. *Macromolecules* **39,** 5987–5994 (2006).
8 O'Reilly, R. K., Joralemon, M. J., Wooley, K. L. & Hawker, C. J. Functionalization of micelles and shell cross-linked nanoparticles using click chemistry. *Chem. Mater.* **17,** 5976–5988 (2005).
9 Thurmond, K. B., Kowalewski, T. & Wooley, K. L. Water-soluble knedel-like structures: the preparation of shell-cross-linked small particles. *J. Am. Chem. Soc.* **118,** 7239–7240 (1996).
10 Tang, C. B., Qi, K., Wooley, K. L., Matyjaszewski, K. & Kowalewski, T. Well-defined carbon nanoparticles prepared from water-soluble shell cross-linked micelles that contain polyacrylonitrile cores. *Angew. Chem., Int. Ed.* **43,** 2783–2787 (2004).
11 Joralemon, M. J., O'Reilly, R. K., Hawker, C. J. & Wooley, K. L. Shell Click-crosslinked (SCC) nanoparticles: a new methodology for synthesis and orthogonal functionalization. *J. Am. Chem. Soc.* **127,** 16892–16899 (2005).
12 Satoh, T. Unimolecular micelles based on hyperbranched polycarbohydrate cores. *Soft Matter* **5,** 1972–1982 (2009).
13 Njikang, G., Gauthier, M. & Li, J. M. Arborescent polystyrene-*g*-poly(2-vinylpyridine) copolymers as unimolecular micelles: solubilization studies. *Polymer* **49,** 1276–1284 (2008).
14 Liu, H. J., Chen, Y., Zhu, D. D., Shen, Z. & Stiriba, S. E. Hyperbranched polyethylenimines as versatile precursors for the preparation of different type of unimolecular micelles. *React. Funct. Polym.* **67,** 383–395 (2007).
15 Liu, H., Jiang, A., Guo, J. & Uhrich, K. E. Unimolecular micelles: Synthesis and characterization of amphiphilic polymer systems. *J. Polym. Sci. Part A: Polym. Chem.* **37,** 703–711 (1999).
16 Thayumanavan, S., Bharathi, P., Sivanandan, K. & Vutukuri, D. R. Towards dendrimers as biomimetic macromolecules. *C. R. Chim.* **6,** 767–778 (2003).
17 Najlah, M., Freeman, S., Attwood, D. & D'Emanuele, A. Synthesis, characterization and stability of dendrimer prodrugs. *Int. J. Pharm.* **308,** 175–182 (2006).
18 Flory, P. J. dendrimer. *J. Am. Chem. Soc.* **74,** 2718 (1952).
19 Hawker, C. J., Wooley, K. L. & Frechet, J. M. J. Unimolecular micelles and globular amphiphiles: dendritic macromolecules as novel recyclable solubilization agents. *J. Chem. Soc. Perkin Trans. I* **12,** 1287–1297 (1993).
20 Uhrich, K. E., Hawker, C. J., Frechet, J. M. J. & Turner, S. R. One-pot synthesis of hyperbranched polyethers. *Macromolecules* **25,** 4583–4587 (1992).
21 Carlmark, A., Hawker, C., Hult, A. & Malkoch, M. New methodologies in the construction of dendritic materials. *Chem. Soc. Rev.* **38,** 352–362 (2009).
22 Hawker, C. J. & Frechet, J. M. J. Monodispersed dendritic polyesters with removable chain ends: a versatile approach to globular macromolecules with chemically reversible polarities. *J. Chem. Soc. Perkin Trans. I* **19,** 2459–2469 (1992).
23 Nguyen, C., Hawker, C. J., Miller, R. D., Huang, E., Hedrick, J. L., Gauderon, R. & Hilborn, J. G. Hyperbranched polyesters as nanoporosity templating agents for organosilicates. *Macromolecules* **33,** 4281–4284 (2000).
24 Hedrick, J. L., Trollsas, M., Hawker, C. J., Atthoff, B., Claesson, H., Heise, A., Miller, R. D., Mecerreyes, D., Jerome, R. & Dubois, P. Dendrimer-like star block and amphiphilic copolymers by combination of ring opening and atom transfer radical polymerization. *Macromolecules* **31,** 8691–8705 (1998).
25 Frechet, J. M. J., Hawker, C. J. & Wooley, K. L. The convergent route to globular dendritic macromolecules: a versatile approach to precisely functionalized 3-dimensional polymers and novel block copolymers. *J. Macromol. Sci. Part A* **A31,** 1627–1645 (1994).
26 Wang, B. B., Zhang, X., Jia, X. R., Li, Z. C., Yan, J. & Wei, Y. Self-assembly of a new class of amphiphilic poly(amidoamine) dendrimers and their electrochemical properties. *J. Polym. Sci. Part A:Polym. Chem.* **43,** 5512–5519 (2005).
27 Percec, V., Peterca, M., Dulcey, A. E., Imam, M. R., Hudson, S. D., Nummelin, S., Adelman, P. & Heiney, P. A. Hollow spherical supramolecular dendrimers. *J. Am. Chem. Soc.* **130,** 13079–13094 (2008).
28 Schenning, A.P.H.J., Peeters, E. & Meijer, E. W. Energy transfer in supramolecular assemblies of oligo(p-phenylene vinylene)s terminated poly(propylene imine) dendrimers. *J. Am. Chem. Soc.* **122,** 4489–4495 (2000).
29 Boas, U., Christensen, J. B. & Heegaard, P. M. H. Dendrimers: design, synthesis and chemical properties. *J. Mater. Chem.* **16,** 3785–3798 (2006).
30 Gillies, E. R. & Frechet, J. M. J. Dendrimers and dendritic polymers in drug delivery. *Drug Discov. Today* **10,** 35–43 (2005).
31 Cloninger, M. J. Biological applications of dendrimers. *Curr. Opin. Chem. Biol.* **6,** 742–748 (2002).
32 Meyers, S. R., Juhn, F. S., Griset, A. P., Luman, N. R. & Grinstaff, M. W. Anionic amphiphilic dendrimers as antibacterial agents. *J. Am. Chem. Soc.* **130,** 14444–14445 (2008).
33 Kim, Y. H. & Webster, O. W. Water-soluble hyperbranched polyphenylene: a unimolecular micelle. *J. Am. Chem. Soc.* **112,** 4592–4593 (1990).
34 Yang, X., Sun, X., Chen, J., Liu, Y. & Wang, X. Study of hyperbranched poly(glycidol) sulfate electrolyte. *J. Appl. Polym. Sci.* **90,** 1185–1190 (2003).
35 Žagar, E., Žigon, M. & Podzimek, S. Characterization of commercial aliphatic hyperbranched polyesters. *Polymer* **47,** 166–175 (2006).
36 Garamus, V. M., Maksimova, T., Richtering, W., Aymonier, C., Thomann, R., Antonietti, L. & Mecking, S. Solution structure of metal particles prepared in unimolecular reactors of amphiphilic hyperbranched macromolecules. *Macromolecules* **37,** 7893–7900 (2004).
37 Sunder, A., Kramer, M., Hanselmann, R., Mulhaupt, R. & Frey, H. Molecular nanocapsules based on amphiphilic hyperbranched polyglycerols. *Angew. Chem., Int. Ed.* **38,** 3552–3555 (1999).
38 Kitajyo, Y., Imai, T., Sakai, Y., Tamaki, M., Tani, H., Takahashi, K., Narumi, A., Kaga, H., Kaneko, N., Satoh, T. & Kakuchi, T. Encapsulation-release property of amphiphilic hyperbranched D-glucan as a unimolecular reverse micelle. *Polymer* **48,** 1237–1244 (2007).
39 Plate, N. A., Valuev, I. L. & Valuev, L. I. Water-soluble polymers with low critical solution temperature (LCST) as carriers for protein drug delivery. *J. Biomater. Sci. Polym. Ed.* **15,** 415–422 (2004).
40 Galaev, I. Y. & Mattiasson, B. Thermoreactive water-soluble polymers, nonionic surfactants, and hydrogels as reagents in biotechnology. *Enzyme Microb. Technol.* **15,** 354–366 (1993).
41 Wang, X. S., Lascelles, S. F., Jackson, R. A. & Armes, S. P. Facile synthesis of well-defined water-soluble polymers via atom transfer radical polymerization in aqueous media at ambient temperature. *Chem. Commun.* 1817–1818 (1999).
42 Schild, H. G. Poly(N-isopropylacrylamide)—experiment, theory and application. *Prog. Polym. Sci.* **17,** 163–249 (1992).
43 Lang, Y. Y., Li, S. M., Pan, W. S. & Zheng, L. Y. Thermo- and pH-sensitive drug delivery from hydrogels constructed using block copolymers of poly(N-isopropylacrylamide) and Guar gum. *J. Drug Delivery Sci. Technol.* **16,** 65–69 (2006).
44 Liu, S. Q., Tong, Y. W. & Yang, Y. Y. Thermally sensitive micelles self-assembled from poly(N-isopropylacrylamide-co-N,N-dimethylacrylamide)-b-poly(D,L-lactide-co-glycolide) for controlled delivers of paclitaxel. *Mol. Biosyst.* **1,** 158–165 (2005).
45 Costa, R. O. R. & Freitas, R. F. S. Phase behavior of poly(N-isopropylacrylamide) in binary aqueous solutions. *Polymer* **43,** 5879–5885 (2002).
46 Wu, C. & Zhou, S. Q. Laser-light scattering study of the phase-transition of poly (N-isopropylacrylamide) in water.1. Single-chain. *Macromolecules* **28,** 8381–8387 (1995).
47 You, Y. Z., Hong, C. Y., Pan, C. Y. & Wang, P. H. Synthesis of a dendritic core-shell nanostructure with a temperature-sensitive shell. *Adv. Mater.* **16,** 1953–1957 (2004).

48 Luo, S. Z., Xu, J., Zhu, Z. Y., Wu, C. & Liu, S. Y. Phase transition behavior of unimolecular micelles with thermoresponsive poly(N-isopropylacrylamide) coronas. *J. Phys. Chem. B* **110,** 9132–9139 (2006).
49 Wang, X., Chen, J., Hong, L. & Tang, X. Synthesis and ionic conductivity of hyperbranched poly(glycidol). *J. Polym. Sci. Part B: Polym. Phys.* **39,** 2225–2230 (2001).
50 Peng, Y., Liu, H. & Zhang, X. Star polystyrene-*b*-hyperbranched polyglycidol: synthesis and ionic conductivity. *J. Polym. Sci. Part A: Polym. Chem.* **47,** 949–958 (2009).
51 Liu, C., Wang, G., Zhang, Y. & Huang, J. Preparation of star polymers of hyperbranched polyglycerol core with multiarms of PS-*b*-PtBA and PS-*b*-PAA. *J. Appl. Polym. Sci.* **108,** 777–784 (2008).
52 Wei, X.- Z., Liu, X.- F., Zhu, B.- K. & Xu, Y.- Y. Membranes of crosslinked hyperbranch polymers and their pervaporation properties. *Desalination* **247,** 647–656 (2009).
53 Zhou, L., Gao, C., Xu, W., Wang, X. & Xu, Y. Enhanced biocompatibility and biostability of CdTe quantum dots by facile surface-initiated dendritic polymerization. *Biomacromolecules* **10,** 1865–1874 (2009).
54 Frey, H. & Haag, R. Dendritic polyglycerol: a new versatile biocompatible material. *Rev. Mol. Biotechnol.* **90,** 257–267 (2002).
55 Burakowska, E. & Haag, R. Dendritic polyglycerol core-double-shell architectures: synthesis and transport properties. *Macromolecules* **42,** 5545–5550 (2009).
56 Tamaki, M., Taguchi, T., Kitajyo, Y., Takahashi, K., Sakai, R., Kakuchi, T. & Satoh, T. LCST-type liquid-liquid and liquid-solid phase transition behaviors of hyperbranched polyglycerol bearing imidazolium salt. *J. Polym. Sci. Part A: Polym. Chem.* **47,** 7032–7042 (2009).
57 Kainthan, R. K. & Brooks, D. E. Unimolecular micelles based on hydrophobically derivatized hyperbranched Polyglycerols: biodistribution studies. *Bioconjugate Chem.* **19,** 2231–2238 (2008).
58 Kainthan, R. K., Mugabe, C., Burt, H. M. & Brooks, D. E. Unimolecular micelles based on hydrophobically derivatized hyperbranched Polyglycerols: ligand binding properties. *Biomacromolecules* **9,** 886–895 (2008).
59 Kainthan, R. K., Janzen, J., Kizhakkedathu, J. N., Devine, D. V. & Brooks, D. E. Hydrophobically derivatized hyperbranched polyglycerol as a human serum albumin substitute. *Biomaterials* **29,** 1693–1704 (2008).
60 Kumar, K. R. & Brooks, D. E. Comparison of hyperbranched and linear polyglycidol unimolecular reverse micelles as nanoreactors and nanocapsules. *Macromol. Rapid Commun.* **26,** 155–159 (2005).
61 Michael Krämer, J.- F. S., Türk, H, Krause, S, Komp, A, Delineau, L, Prokhorova, S, Kautz, H & Haag, R pH-responsive molecular nanocarriers based on dendritic core-shell architectures. *Angew. Chem., Int. Ed.* **41,** 4252–4256 (2002).
62 Kojima, C., Yoshimura, K., Harada, A., Sakanishi, Y. & Kono, K. Synthesis and characterization of hyperbranched poly(glycidol) modified with ph- and temperature-sensitive groups. *Bioconjugate Chem.* **20,** 1054–1057 (2009).
63 Wilms, D., Stiriba, S.- E. & Frey, H. Hyperbranched polyglycerols: from the controlled synthesis of biocompatible polyether polyols to multipurpose applications. *Acc. Chem. Res.* **43,** 129–141 (2010).
64 Xu, H., Luo, S. H., Shi, W. F. & Liu, S. Y. Two-stage collapse of unimolecular micelles with double thermoresponsive coronas. *Langmuir* **22,** 989–997 (2006).
65 Wu, C. & Xia, K. Q. Incorporation of a differential refractometer into a laser light-scattering spectrometer. *Rev. Sci. Instrum.* **65,** 587–590 (1994).
66 agar, E. & igon, M. Characterization of a commercial hyperbranched aliphatic polyester based on 2,2-bis(methylol)propionic acid. *Macromolecules* **35,** 9913–9925 (2002).
67 Wu, C. & Zhou, S. Q. First observation of the molten globule state of a single homopolymer chain. *Phys. Rev. Lett.* **77,** 3053–3055 (1996).
68 Zhang, G. Z. Study on conformation change of thermally sensitive linear grafted poly (N-isopropylacrylamide) chains by quartz crystal microbalance. *Macromolecules* **37,** 6553–6557 (2004).
69 Liu, G. M., Cheng, H., Yan, L. F. & Zhang, G. Z. Study of the kinetics of the pancake-to-brush transition of poly(N-isopropylacrylamide) chains. *J. Phys. Chem. B* **109,** 22603–22607 (2005).
70 Zhang, G. Z. & Wu, C. Quartz crystal microbalance studies on conformational change of polymer chains at interface. *Macromol. Rapid Commun.* **30,** 328–335 (2009).
71 Yim, H., Kent, M. S., Satija, S., Mendez, S., Balamurugan, S. S., Balamurugan, S. & Lopez, G. P. Evidence for vertical phase separation in densely grafted, high-molecular-weight poly(N-isopropylacrylamide) brushes in water. *Phys. Rev. E* **72,** 051801 (2005).
72 Balamurugan, S. S., Bantchev, G. B., Yang, Y. M. & McCarley, R. L. Highly water-soluble thermally responsive poly(thiophene)-based brushes. *Angew. Chem., Int. Ed.* **44,** 4872–4876 (2005).
73 Yim, H., Kent, M. S., Satija, S., Mendez, S., Balamurugan, S. S., Balamurugan, S. & Lopez, C. P. Study of the conformational change of poly(N-isopropylacrylamide)-grafted chains in water with neutron reflection: molecular weight dependence at high grafting density. *J. Polym. Sci. Part B: Polym. Phys.* **42,** 3302–3310 (2004).
74 Yim, H., Kent, M. S., Mendez, S., Balamurugan, S. S., Balamurugan, S., Lopez, G. P. & Satija, S. Temperature-dependent conformational change of PNIPAM grafted chains at high surface density in water. *Macromolecules* **37,** 1994–1997 (2004).
75 Balamurugan, S., Mendez, S., Balamurugan, S. S., O'Brien, M. J. & Lopez, G. P. Thermal response of poly(N-isopropylacrylamide) brushes probed by surface plasmon resonance. *Langmuir* **19,** 2545–2549 (2003).
76 Žagar, E. & Žigon, M. Molar mass distribution of a commercial aliphatic hyperbranched polyester based on 2,2-bis(methylol)propionic acid. *J. Chromatogr. A* **1034,** 77–83 (2004).
77 Halperin, A., Tirrell, M. & Lodge, T. P. Tethered chains in polymer microstructures. *Adv. Polym. Sci.* **100,** 31–71 (1992).
78 Teraoka, I. *Polymer Solutions: An Introduction to Physical Properties* (John Wiley & Sons, New York, 2002).